



## 车排子凸起东翼中生界原油生物降解程度评价

苏蕾, 常象春, 徐佑德, 柳忠泉, 史兵兵

### 引用本文:

苏蕾, 常象春, 徐佑德, 柳忠泉, 史兵兵. 车排子凸起东翼中生界原油生物降解程度评价[J]. 沉积学报, 2024, 42(4): 1422-1432.

SU Lei, CHANG XiangChun, XU YouDe, et al. Evaluation of the Biodegradation of Mesozoic Crude Oils in the Eastern Chepaizi Uplift[J]. *Acta Sedimentologica Sinica*, 2024, 42(4): 1422-1432.

### 相似文章推荐 (请使用火狐或IE浏览器查看文章)

Similar articles recommended (Please use Firefox or IE to view the article)

#### 二连盆地宝勒根陶海凹陷烃源岩生物标志化合物特征与油源对比

Biomarker Characteristics of Source Rocks and Oil Source Correlation in Baolegentaohai Sag, Erlian Basin

沉积学报. 2020, 38(2): 451-462 <https://doi.org/10.14027/j.issn.1000-0550.2019.034>

#### 柴达木盆地东坪地区一类新的原油及其地球化学特征

A New Kind of Crude Oils and the Geochemical Characteristics in the Dongping Area, Qaidam Basin

沉积学报. 2018, 36(4): 829-841 <https://doi.org/10.14027/j.issn.1000-0550.2018.074>

#### 庙西凹陷严重生物降解原油序列中三环萜烷的异常分布成因初探

Abnormal Distributions of Tricyclic Terpanes and Its Genesis in Severely Biodegraded Oils from the Miaoxi Depression, Bohai Bay Basin

沉积学报. 2017, 35(1): 193-202 <https://doi.org/10.14027/j.cnki.cjxb.2017.01.019>

#### 查干凹陷下白垩统稠油地球化学特征及成因分析

Geochemistry and Origin of Heavy Oil in Lower Cretaceous of Chagan Depression

沉积学报. 2015, 33(6): 1265-1274 <https://doi.org/10.14027/j.cnki.cjxb.2015.06.019>

#### 鄂尔多斯盆地陇东地区长9油层组油源分析

Oil-source Analysis for Chang-9 Subsection (Upper Triassic) of Eastern Gansu Province in Ordos Basin

沉积学报. 2015, 33(5): 1023-1032 <https://doi.org/10.14027/j.cnki.cjxb.2015.05.018>

# 车排子凸起东翼中生界原油生物降解程度评价

苏蕾<sup>1</sup>,常象春<sup>1</sup>,徐佑德<sup>2</sup>,柳忠泉<sup>2</sup>,史兵兵<sup>1</sup>

1. 山东科技大学地球科学与工程学院, 山东青岛 266590

2. 中国石化胜利油田分公司勘探开发研究院, 山东东营 257015

**摘要** 【目的】车排子凸起中生界稠油资源丰富,但原油生物降解严重,制约了勘探进程。【方法】为明确车排子凸起东翼中生界原油的生物降解程度,对车排子凸起东翼侏罗纪和白垩纪储层样品抽提出的饱和烃和芳香烃进行了气相色谱-质谱(GC-MS)分析,采用分子地球化学指标,对其进行定性与定量评价。【结果】通过聚类分析,将原油分为I、II、III、IV四类族群。PM(Peters and Moldowan)法分析结果表明I<sub>1</sub>类和II<sub>1</sub>类原油的生物降解程度达PM7,I<sub>2</sub>类和IV类原油的生物降解程度为PM8;II<sub>2</sub>类和III<sub>1</sub>类原油的生物降解程度为PM9,III<sub>2</sub>类原油生物降解程度为PM9+。基于优化的Manco法求得的MN<sub>1</sub>值介于19 693~215 623,I类原油的MN<sub>2</sub>值介于769~919,II类原油的MN<sub>2</sub>值介于768~907,III类原油的MN<sub>2</sub>值介于906~954,IV类原油的MN<sub>2</sub>值介于774~817。同一原油族群的Manco数与原油密度、黏度、非烃和沥青质含量均呈现良好的正相关性,与总烃呈现良好的负相关性。优化的Manco法成功厘定了生物降解程度在PM7-PM9+的储层样品,与PM等级评价具有一致性。【结论】与PM法相比,优化的Manco法对原油生物降解的识别分辨率更高。通过PM法定性评价和优化Manco法定量评价相结合,可以很好地揭示原油物性的变化,对稠油区的油气勘探有重要的指导作用。

**关键词** 生物降解;PM法;优化Manco法;中生界;车排子凸起

**第一作者简介** 苏蕾,女,1998年出生,硕士研究生,油气地球化学,E-mail:sulei17866835736@163.com

**通信作者** 常象春,男,教授,油气地球化学,E-mail:xcchang@sina.com

**中图分类号** P618.13 **文献标志码** A

## 0 引言

全球范围内原油的生物降解现象较为普遍,大量研究表明生物降解对原油物理性质及组分都有影响。经过生物降解作用,原油黏度增加,非烃、沥青质、硫和金属离子含量增加,酸值上升<sup>[1-5]</sup>。原油生物降解的评价方法主要有PM法和Manco法。PM法是Peters *et al.*<sup>[3]</sup>基于化合物类型对微生物侵蚀的抵抗能力建立的定性评价生物降解的方法,可将生物降解等级分为10个级别(PM1~PM10),Wenger *et al.*<sup>[5]</sup>根据降解程度又补充说明了描述性的术语在PM法中的赋值规则:轻微(PM1~PM3);中等(PM4~PM5);严重(PM6~PM7);很严重(PM8~PM9);强烈(PM10)。Manco法是Larter *et al.*<sup>[6]</sup>提出的一种定量评价生物降解的方法,Manco法选取了8种抗生物降解能力逐渐增强的化合物(烷基甲苯、萘+甲基萘、C<sub>2</sub>萘、C<sub>3</sub>萘、C<sub>4</sub>萘、C<sub>0,2</sub>菲、甲基二苯并噻吩和甾烷),并按照8种化合

物的降解程度划分为5个等级,即完全未降解(Manco赋值为0),只发生轻微降解(Manco赋值为1),化合物不完全降解(Manco赋值为3)和介于二者之间的(Manco赋值为2),完全降解(通常化合物被全部消耗,Manco赋值为4)。通过Manco法获取的MN<sub>1</sub>和MN<sub>2</sub>值可以清晰地区别介于PM4~PM8的原油,提高了生物降解程度评价的精度。但Manco法只适用于区别介于PM4~PM8的原油,不适用于生物降解程度在PM8以上的原油。但Larter *et al.*<sup>[6]</sup>也提出了可以通过优化Manco法中的赋值参数,构建适用于更高生物降解程度的原油评价。

准噶尔盆地是我国西部油气资源最为丰富的含油气盆地之一,车排子凸起石炭系是主要的产油层。近年来在车排子凸起中生界也发现良好的油气显示,但此处的油气来源仍存在争议,生物降解作用造成的油源对比困难是其缘由之一,因而研究车排子凸起中生界原油生物降解情况对深化油气勘探评价

具有重要意义。Chang *et al.*<sup>[7]</sup>研究发现车排子凸起石炭系原油的生物降解程度可达PM9+,由于车排子凸起的中生界原油与石炭系原油具有相似的地球化学特征,考虑到中生界原油也存在严重降解的可能性,本文利用PM法和优化的Manco法对准噶尔盆地车排子凸起中生界原油生物降解程度进行定性和定量的综合评价。

## 1 地质背景

车排子凸起位于准噶尔盆地的西部隆起南段,面积约 $1.08 \times 10^4 \text{ km}^2$ <sup>[8]</sup>,是一个继承性古隆起,形成于海西晚期构造运动早期<sup>[9-11]</sup>。西面和北面邻近扎伊尔山,南面为四棵树凹陷,向东以红车断裂带与沙湾凹陷相接,整体上呈三角形(图1a<sup>[12]</sup>)。准噶尔盆地车排子凸起自晚石炭世已开始发育,依次经历了强挤压—弱挤压—较弱挤压—弱伸展的演化过程,其构造演化可划分为初始发育(C<sub>3</sub>~P)、持续隆升(T~J)、稳定埋深(K~E)和局部伸展掀斜(N~Q)4个阶段<sup>[8]</sup>。车排子凸起基底为石炭系,自下而上发育侏罗系、白垩系、古近系、新近系和第四系,缺失二叠系和三叠系。各时代地层厚度总体较薄,向西北向尖灭<sup>[13]</sup>。车排子凸起断层发育,保存了多期构造运动叠加的构造格局,且油气源条件优越,成为盆地内重要的油气聚集区<sup>[8]</sup>。车排子凸起拥有3套含油储层、6套烃源岩(石炭系、中一下二叠系、上三叠统、中一下侏罗系、白垩系、古近系)、多期油气充注、原油物性多变<sup>[14]</sup>。近年来,在车排子凸起白垩系、侏罗系、古近系和新近系获得高产工业油气流,显示良好的油气勘探前景<sup>[15]</sup>。

## 2 样品与实验

本次研究共采集车排子凸起东翼中生界10口井的含油储层岩石样品,其中包括侏罗系P1井;白垩系P1井、P60井、P68井、P604井、P606井、P607井、P609井、P624井、P629井、P646井(图1b)。

将适量储层岩石样品(10 g)磨成100目的粉末,用正己烷和二氯甲烷进行萃取获得抽提物,使用常规硅胶和氧化铝柱进行柱层析,用正己烷和二氯甲烷得到脂肪族和芳香族组分。使用安捷伦7890A GC/5977 MSD仪器对脂肪族和芳香族组分进行了气相色谱—质谱法(GC-MS)分析。脂肪族组分的GC温度操作条件为:从100 ℃(1 min)升至220 ℃,速率为4 ℃/min,然后以2 ℃/min的速率升至300 ℃(保温5 min);芳香族组分的GC温度操作条件为:从80 ℃(1 min)升至300 ℃(保温15 min),速率为3 ℃/min。MS(质谱)条件如下:电子碰撞(EI)电离模式,70 eV电子能量,300 mA发射电流,50~550 amu/s扫描范围。

## 3 结果与讨论

### 3.1 原油物性

本实验选取的侏罗系和白垩系的样品都集中在车排子凸起东翼。侏罗系原油的密度在 $0.945 \sim 0.988 \text{ g} \cdot \text{cm}^{-3}$ ,黏度在 $592 \sim 5\ 879 \text{ mPa} \cdot \text{s}$ <sup>[16]</sup>;白垩系原油的密度在 $0.945 \sim 0.980 \text{ g} \cdot \text{cm}^{-3}$ ,黏度在 $592 \sim 37\ 192 \text{ mPa} \cdot \text{s}$ (表1)。侏罗系原油和白垩系原油均为重质稠油,原油族组成中非烃和沥青质含量介于28.57%~75.48%,占绝对优势(图2)。

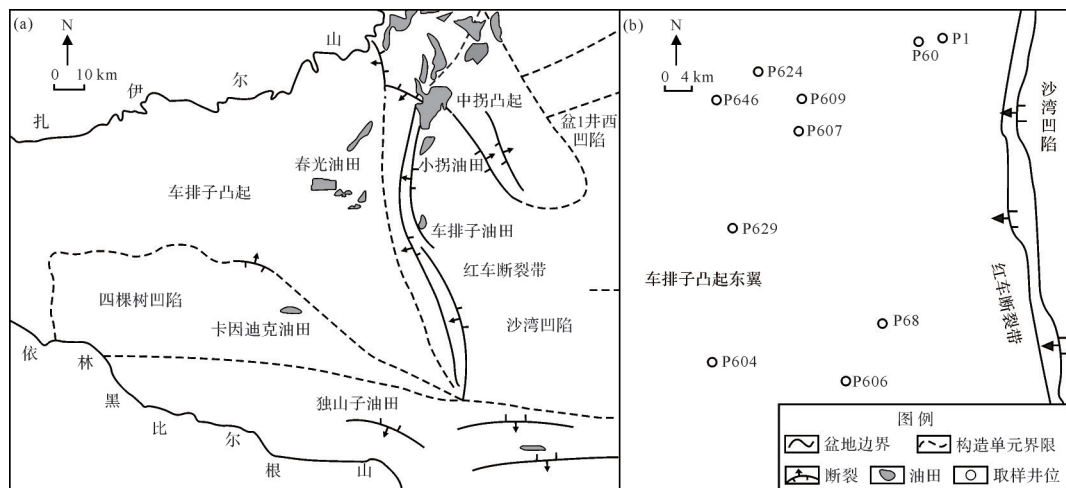


图1 车排子凸起构造分区<sup>[12]</sup>及井位分布图

Fig.1 Structural units and well location in the Chepaizi uplift

表1 原油物性参数表<sup>[16]</sup>  
Table 1 Physical property parameters of crude oil<sup>[16]</sup>

井号	深度/m	层位	饱和烃/%	芳烃/%	非烃+沥青质/%	饱/芳	总烃/%	密度/g·cm <sup>-3</sup>	黏度/mPa·s
P1	721.5	K	35.65	27.79	36.56	1.28	63.44	0.945 0	592
P1	748.5	K	57.29	9.72	32.99	5.89	67.01	0.946 0	2 301
P1	751.2	K	41.73	8.65	49.62	4.83	50.38	0.946 0	2 301
P1	756.8	J	35.31	14.89	49.80	2.37	50.20	0.945 0	592
P1	757.0	J	37.81	11.51	50.68	3.29	49.32	0.945 0	592
P1	761.6	J	16.35	8.17	75.48	2.00	24.52	0.988 0	5 879
P1	766.5	J	25.21	15.29	59.50	1.65	40.50	0.988 0	5 879
P1	781.5	J	42.86	28.57	28.57	1.50	71.43	0.945 0	592
P604	682.9	K	27.02	16.43	56.55	1.64	43.45		
P606	960.5	K	27.32	17.56	55.12	1.56	44.88	0.956 8	2 354
P607	349.1	K	29.84	18.33	51.83	1.63	48.17	0.975 0	29 664
P646	256.5	K	22.89	10.44	66.67	2.19	33.33	0.962 9	1 830
P60	579.9	K	40.96	18.08	40.96	2.27	59.04	0.963 5	8 978
P68	930.1	K	42.34	18.92	38.74	2.24	61.26		
P609	310.1	K	33.94	24.09	41.97	1.41	58.03	0.980 2	37 192
P624	278.0	K	37.33	21.20	41.47	1.76	58.53		
P629	385.0	K	12.96	26.13	60.91	0.50	39.09		

3.2 原油族群划分

来源于同一烃源层或同一油源区的原油定义为同一原油族群(Oil Population)。聚类分析(HCA)是将研究对象分为相对同质的群组的统计分析技术,可以根据不同变量计算出的相似距离将研究样本分为不同的组。选取与三环萜烷(TT)、四环萜烷(Tet)、三芳甾烷(TAS)相关的9个抗生物降解极强的

生物标志物参数:  $(C_{19}TT+C_{20}TT)/(C_{23}TT+C_{24}TT)$ ,  $C_{19}TT/C_{23}TT$ ,  $C_{23}TT/C_{21}TT$ ,  $C_{22}TT/C_{21}TT$ ,  $C_{24}TT/C_{23}TT$ , ETR,  $C_{24}Tet/C_{26}TT$ ,  $C_{27}TAS/C_{28}TAS$  (20R),  $C_{26}TAS/C_{28}TAS$  (20S),采用聚类分析对车排子凸起东翼中生界原油样品进行划分(表2)。在聚类谱系图中(图3),根据不同变量计算出的相似距离,可以分为 I、II、III、IV 四类族群。

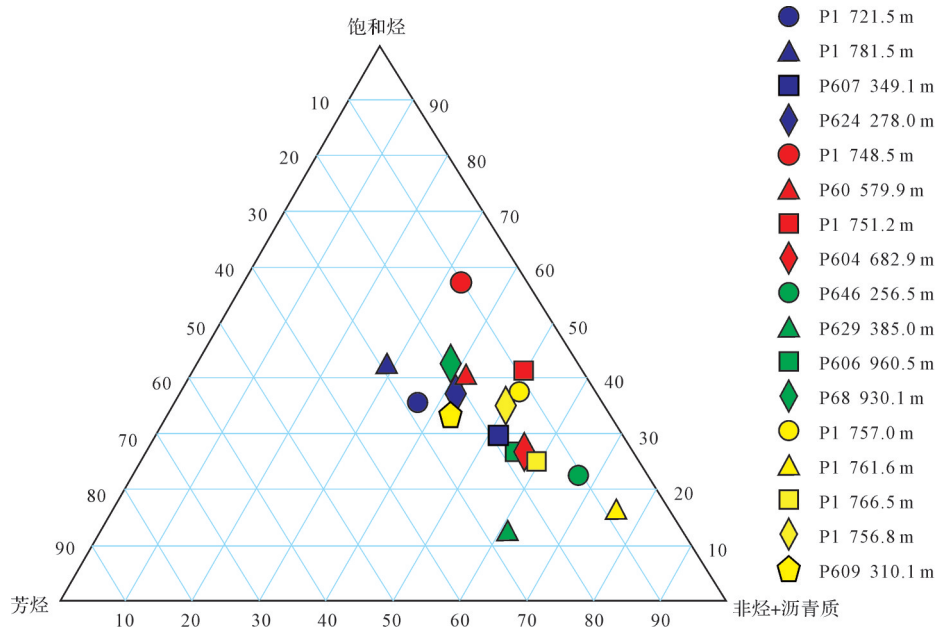


图2 原油族组成三角图  
Fig.2 Ternary diagram of oil bulk compositions

表2 原油地球化学参数及族群划分结果

Table 2 Geochemical parameters of crude oil and population identification

井号	层系	深度/m	L1	L2	L3	L4	L5	L6	L7	L8	L9	族群
P1	K	721.5	0.43	0.17	2.08	0.42	0.33	0.87	0.30	1.15	0.56	I
P1	J	781.5	0.44	0.15	1.05	0.28	0.53	0.89	0.36	1.42	0.27	I
P607	K	349.1	0.47	0.15	1.10	0.43	0.34	0.87	0.35	1.12	0.11	I
P624	K	278.0	0.97	0.35	0.75	0.17	0.33	0.88	0.41	1.32	0.14	I
P1	K	748.5	0.53	0.18	1.04	0.26	0.50	0.86	0.33	0.36	0.67	II
P1	K	751.2	0.72	0.18	0.84	0.23	0.50	0.90	0.29	0.68	1.55	II
P60	K	579.9	0.21	0.06	1.17	0.30	0.50	0.77	0.30	0.36	1.66	II
P604	K	682.9	0.43	0.20	1.87	0.73	0.52	0.87	0.25	1.13	2.35	II
P68	K	930.1	1.58	0.47	0.60	0.22	0.55	0.80	0.41	2.50	0.75	III
P606	K	960.5	1.49	0.43	0.74	0.18	0.37	0.80	0.44	1.02	1.21	III
P629	K	385.0	1.01	0.57	2.19	0.74	0.35	0.83	0.35	1.39	0.89	III
P646	K	256.5	0.88	0.50	2.36	0.75	0.30	0.82	0.19	0.98	0.96	III
P1	J	756.8	0.22	0.12	2.81	0.62	0.27	0.81	0.33	0.33	0.81	IV
P1	J	757.0	0.27	0.15	5.96	1.14	0.29	0.80	0.30	0.62	1.38	IV
P1	J	761.6	0.12	0.10	8.80	1.21	0.30	0.79	0.34	0.91	0.52	IV
P1	J	766.5	0.42	0.18	4.10	0.84	0.28	0.80	0.33	0.86	0.54	IV
P609	K	310.1	0.54	0.17	0.88	0.26	0.37	0.78	0.33	1.17	0.21	IV

注: L1= (C<sub>19</sub>TT+C<sub>20</sub>TT)/(C<sub>23</sub>TT+C<sub>24</sub>TT); L2= C<sub>19</sub>TT/C<sub>23</sub>TT; L3= C<sub>23</sub>TT/C<sub>21</sub>TT; L4= C<sub>22</sub>TT/C<sub>21</sub>TT; L5= C<sub>24</sub>TT/C<sub>23</sub>TT; L6= ETR; L7= C<sub>24</sub>Tet/C<sub>26</sub>TT; L8= C<sub>27</sub>TAS/C<sub>28</sub>TAS(20R); L9= C<sub>26</sub>TAS/C<sub>28</sub>TAS(20S)。

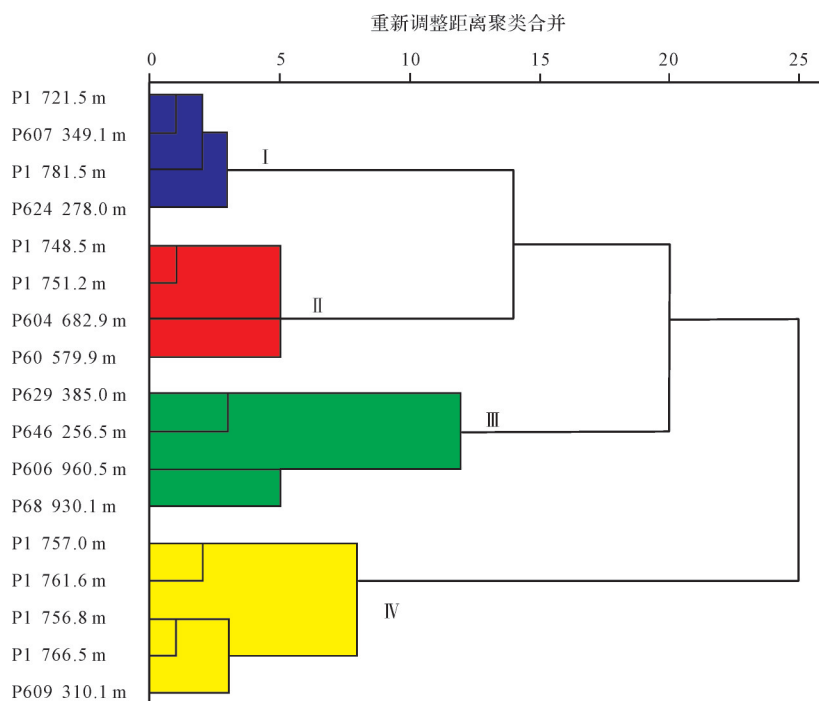


图3 原油族群划分聚类谱系图

Fig.3 Dendrogram of cluster analysis of the crude oil populations

### 3.3 PM法定性评价生物降解

车排子凸起东翼中生界储层样品的饱和烃总离子流图(TIC)具有高度相似特征,谱图基线呈现明显的“鼓包”,反映色谱分析未分辨的复杂混合物,主要是环烷烃及异构烷烃成分,称之为 UCM 峰

(Unresolved Complex Mixture),通常作为原油遭受生物降解作用的标志。通过对饱和烃总离子流谱图、反映萘烷系列化合物的 *m/z* 191 谱图、反映甾烷系列化合物的 *m/z* 217 谱图和反映芳香甾烷系列化合物的 *m/z* 231 谱图的分析,发现车排子凸起原油呈现不同

的生物降解特征,依据 Peters 和 Moldowan 在 1993 年提出的 PM 法<sup>[3]</sup>和 Wenger *et al.*<sup>[5]</sup>在 2002 年补充说明的描述性的术语在 PM 法中的赋值规则,对车排子凸起原油生物降解程度进行评价。

I 类原油可细分为 I<sub>1</sub>类原油: P1 (781.5 m)、P1 (721.5 m) 和 I<sub>2</sub>类原油: P607 (349.1 m)、P624 (278 m)。I<sub>1</sub>类原油饱和烃的 TIC 图上可见显著的 UCM 鼓包, 仅可检测到少量的正构烷烃化合物(图 4a)。m/z 191 谱图中, 藿烷以 C<sub>30</sub>H 为主峰, 三环萜烷呈现 C<sub>23</sub>TT 优势, 三环萜烷未发生降解, 说明降解程度未达 PM8<sup>[17]</sup>(图 4a)。m/z 217 谱图中, 甾烷发生实质性消耗, 说明生物降解程度已达 PM7<sup>[3]</sup>(图 4a)。m/z 231 谱图中, 萘和菲基本上完全消除, 三芳甾烷未发生降解(图 4a), 原油生物降解程度定为 PM7。I<sub>2</sub>类原油饱和烃的 TIC 图上可见显著的 UCM 鼓包, 仅可检测到少量的正构烷烃化合物(图 4b), m/z 191 谱图中, 25-NH(25-降藿烷)消失, 藿烷严重消耗, 说明生物降解程度可达 PM8<sup>[3]</sup>。更耐生物降解的三环萜烷初步消耗, 三环萜烷呈现 C<sub>21</sub>TT 优势, 表明生物降解等级已达 PM8<sup>[17]</sup>(图 4b)。m/z 217 谱图中, 甾烷基本上完全消除, 孕甾烷和升孕甾烷丰度远高于甾烷(图 4b)。m/z 231 谱图中, 三芳甾烷未发生降解(图 4b), 原油生物降解程度定为 PM8。

II 类原油可细分为 II<sub>1</sub>类原油: P1 (748.5 m)、P1 (751.2 m) 和 II<sub>2</sub>类原油: P60 (579.9 m) 和 P604 (682.9 m)。II<sub>1</sub>类原油饱和烃的 TIC 图上可见显著的 UCM 鼓包, 仅可检测到少量的正构烷烃化合物(图 4c)。m/z 191 谱图中, 藿烷以 C<sub>30</sub>H 为主峰。三环萜烷呈现 C<sub>23</sub>TT 优势, 三环萜烷未发生降解, 说明降解程度未达 PM8<sup>[17]</sup>(图 4c)。m/z 217 谱图中, 甾烷发生实质性消耗, 说明生物降解程度已达 PM7<sup>[3]</sup>(图 4c)。m/z 231 谱图中, 萘和菲基本上完全消除, 三芳甾烷未发生降解(图 4c), 原油生物降解程度定为 PM7。II<sub>2</sub>类原油饱和烃的 TIC 图上难以检测到可分辨的生物标志物(图 4d)。m/z 191 谱图中, 藿烷系列已完全消除, 三环萜烷系列发生实质性的消耗但丰度仍高于藿烷系列(图 4d)。m/z 217 谱图中, 重排甾烷发生实质性消耗, 说明生物降解程度达 PM9<sup>[3]</sup>(图 4d)。芳烃的 m/z 231 谱图中, 三芳甾烷未发生降解(图 4d), 原油生物降解程度定为 PM9。

III 类原油可细分为 III<sub>1</sub>类原油: P629 (385 m)、P68 (930.1 m)、P606 (960.5 m) 和 III<sub>2</sub>类原油: P646

(256.5 m)。III<sub>1</sub>类原油饱和烃的 TIC 图上难以检测到可分辨的生物标志物(图 4e)。m/z 191 谱图中, 藿烷系列已完全消除, 三环萜烷系列发生实质性的消耗但丰度仍高于藿烷系列(图 4e)。m/z 217 谱图中, 重排甾烷发生实质性消耗, 说明生物降解程度达 PM9<sup>[3]</sup>(图 4e)。m/z 231 谱图中, 三芳甾烷未发生降解(图 4e), 原油生物降解程度定为 PM9。III<sub>2</sub>类原油饱和烃的 TIC 图上难以检测到可分辨的生物标志物(图 4f)。m/z 191 谱图中, 三环萜烷基本上完全消除, 与已完全消耗的藿烷系列丰度相当(图 4f)。m/z 217 谱图中, 重排甾烷基本上完全消除, 孕甾烷和升孕甾烷发生实质性降解(图 4f), 孕甾烷和升孕甾烷要比规则甾烷和重排甾烷的抗生物降解能力更强<sup>[18]</sup>, 说明生物降解程度大于 PM9<sup>[3]</sup>。m/z 231 谱图中, 三芳甾烷初步消耗(图 4f), 芳香化的甾族烃是抵抗生物降解能力最强的化合物, 在生物降解等级达 PM10 之外的几乎所有原油中仍然能保存不变<sup>[17]</sup>, 原油生物降解程度定为 PM9+。

IV 类原油包括 P1 (756.8 m)、P1 (757 m)、P1 (761.6 m)、P1 (766.5 m) 和 P609 (310.1 m)。饱和烃的 TIC 图上难以检测到可分辨的生物标志物(图 4g)。m/z 191 谱图中, 25-NH 消失, 藿烷严重消耗(图 4g), 说明生物降解程度可达 PM8<sup>[3]</sup>。更耐生物降解的三环萜烷初步消耗(图 4g), 表明着生物降解等级已达 PM8<sup>[17]</sup>。m/z 217 谱图中, 甾烷基本上完全消除, 孕甾烷和升孕甾烷丰度远高于甾烷(图 4g)。芳烃的 m/z 231 谱图中, 三芳甾烷未发生降解(图 4g), 原油生物降解程度定为 PM8。

### 3.4 基于优化 Manco 法的降解程度定量评价

基于 Manco 法的学术思想, 选取了 8 种对微生物降解作用的敏感性不同且呈现递减关系的化合物, 来优化 Manco 法的赋值参数, 对原油生物降解程度进行定量分析。8 种化合物的参数向量覆盖全降解区间(PM0~PM10), 具体为: (1) 正构烷烃(m/z 85); (2) 萘和烷基萘(m/z 128、142、156、170、184、198); (3) 烷基二苯并噻吩(m/z 198、212、226); (4) C<sub>0-3</sub>菲(m/z 178、192、206、220); (5) 五环三萜类(m/z 191、177、205); (6) 甾烷(m/z 217、218、259); (7) 三环萜类(m/z 191、177); (8) 三芳甾类(m/z 231、245)。对所有样品进行分析评价, 定性划分出 8 种化合物的降解程度, 通过以下公式计算 MN<sub>1</sub>(Manco Number 1)和 MN<sub>2</sub>(Manco Number 2)<sup>[6]</sup>。

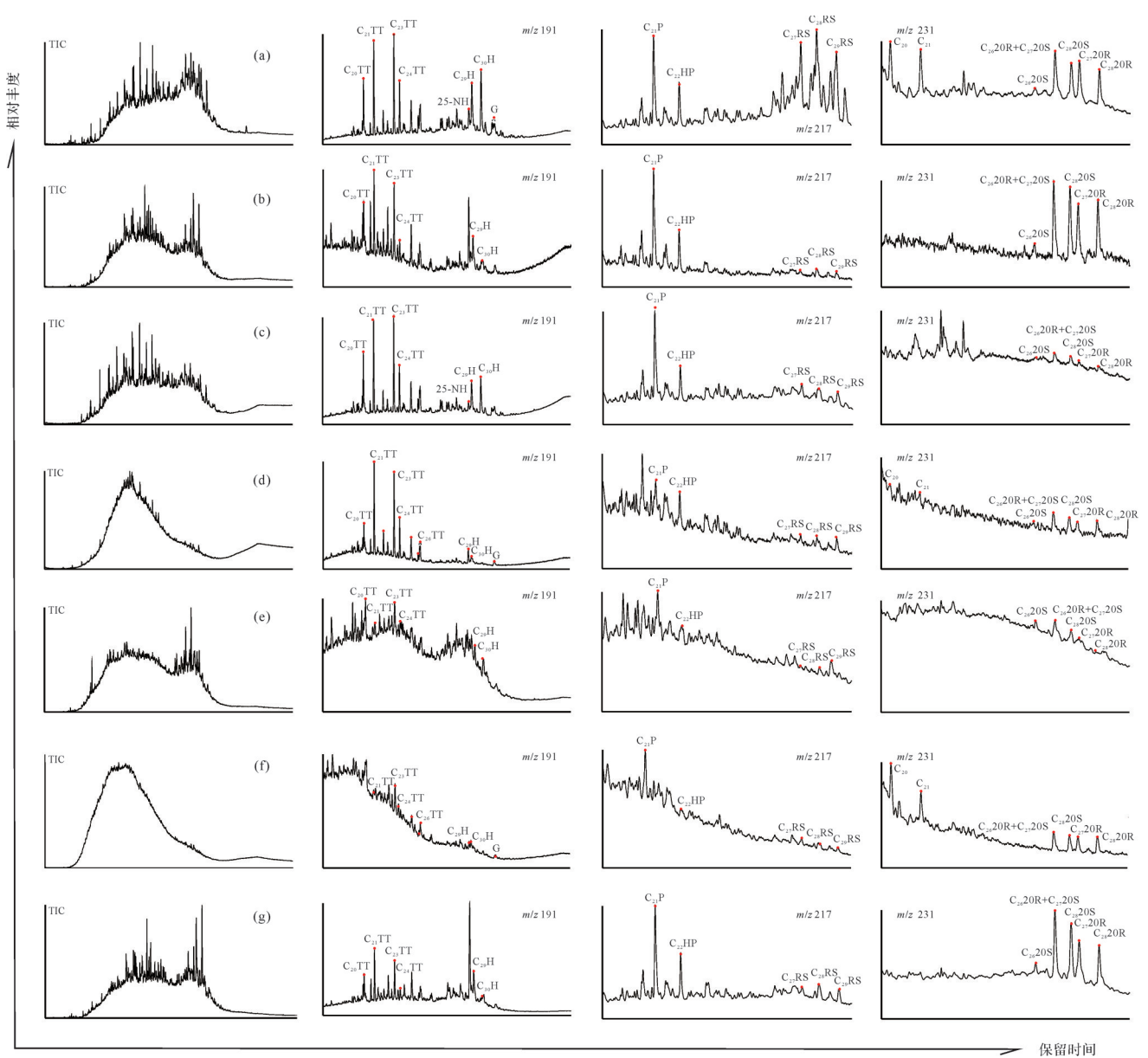


图4 车排子凸起部分样品生物降解程度评价  
 (a)P1井,781.5 m;(b) P607井,349.1 m;(c)P1井,751.2 m;(d)P60井,579.9 m;(e)P629井,385.0 m;(f)P646井,256.5 m;(g)P609井,310.1 m  
 Fig.4 Evaluation of biodegradation level of representative samples from the Chepaizi uplift

$$MN_1 = \sum m_i 5^i \quad (1)$$

$$MN_2 = [n + \log_5(MN_1) \times (S_{max} - 1)]/n \quad (2)$$

式中:m是指八个向量元素(0~4)中每个元素的Manco分数,i表示类号(0~7),n是复合类的数量。 $S_{max}$ 是 $MN_2$ 的最大值,被指定为1 000,以避免与当前存在的尺度混淆,并在使用整数时确保在不同的生物降解水平下有足够的分辨率。结果如表3。

由表3可知,优化的Manco法求得的 $MN_1$ 值介于19 693~215 623, $MN_2$ 值介于768~954,在同一原油族群内, $MN_1$ 值和 $MN_2$ 值随着生物降解程度增大而

增大。I类原油的 $MN_2$ 值介于769~919,II类原油的 $MN_2$ 值介于768~907,III类原油的 $MN_2$ 值介于906~954,IV类原油的 $MN_2$ 值介于774~817。在同一原油族群内,Manco数与原油密度(图5a)、黏度(图5b)、非烃和沥青质含量(图5c)均呈现良好的正相关性,Manco数与总烃呈现良好的负相关性(图5d)。研究表明,生物降解过程降低了饱和烃和芳香烃的含量,并丰富了非烃和沥青质的含量,从而导致原油密度的增加<sup>[19-22]</sup>。比较例外的是,III类原油中生物降解程度更高的P646井样品,其黏度却低于P606井样品。

表3 基于优化Manco法求取的 $MN_1$ 和 $MN_2$ 值  
Table 3  $MN_1$  and  $MN_2$  values calculated by improved Manco method

族群	井号	深度/m	层位	PM	NA	N+MN	MDBT	P+MP	H+25-NH	S	TT	TAS	$MN_1$	$MN_2$
I <sub>1</sub>	P1	721.5	K	7	3	3	2	2	2	1	2	0	35 943	815
I <sub>1</sub>	P1	781.5	J	7	3	4	4	4	1	1	1	0	19 998	769
I <sub>2</sub>	P624	278.0	K	8	2	2	3	2	2	1	3	0	51 587	843
I <sub>2</sub>	P607	349.1	K	8	3	4	4	4	3	3	3	1	136 873	919
II <sub>1</sub>	P1	748.5	K	7	3	3	2	2	1	1	1	0	19 693	768
II <sub>2</sub>	P60	579.9	K	9	4	4	3	4	3	2	2	1	118 099	907
III <sub>1</sub>	P606	960.5	K	9	4	2	3	4	4	1	2	1	115 589	906
III <sub>1</sub>	P629	385.0	K	9	3	4	3	4	4	3	3	1	137 473	919
III <sub>2</sub>	P646	256.5	K	9+	3	4	4	4	4	3	3	2	215 623	954
IV	P1	757.0	J	8	4	2	3	4	3	1	1	0	21 214	774
IV	P1	761.6	J	8	3	4	3	4	3	1	1	0	21 223	774
IV	P1	766.5	J	8	3	4	3	4	3	1	2	0	36 848	817

注: NA. 正构烷烃; N+MN. 萘+烷基萘; MDBT. 烷基二苯并噻吩; P+MP. 菲+烷基菲; H+25-NH. 藿烷+25-降藿烷; S. 甾烷; TT. 三环萜烷; TAS. 三芳甾烷。

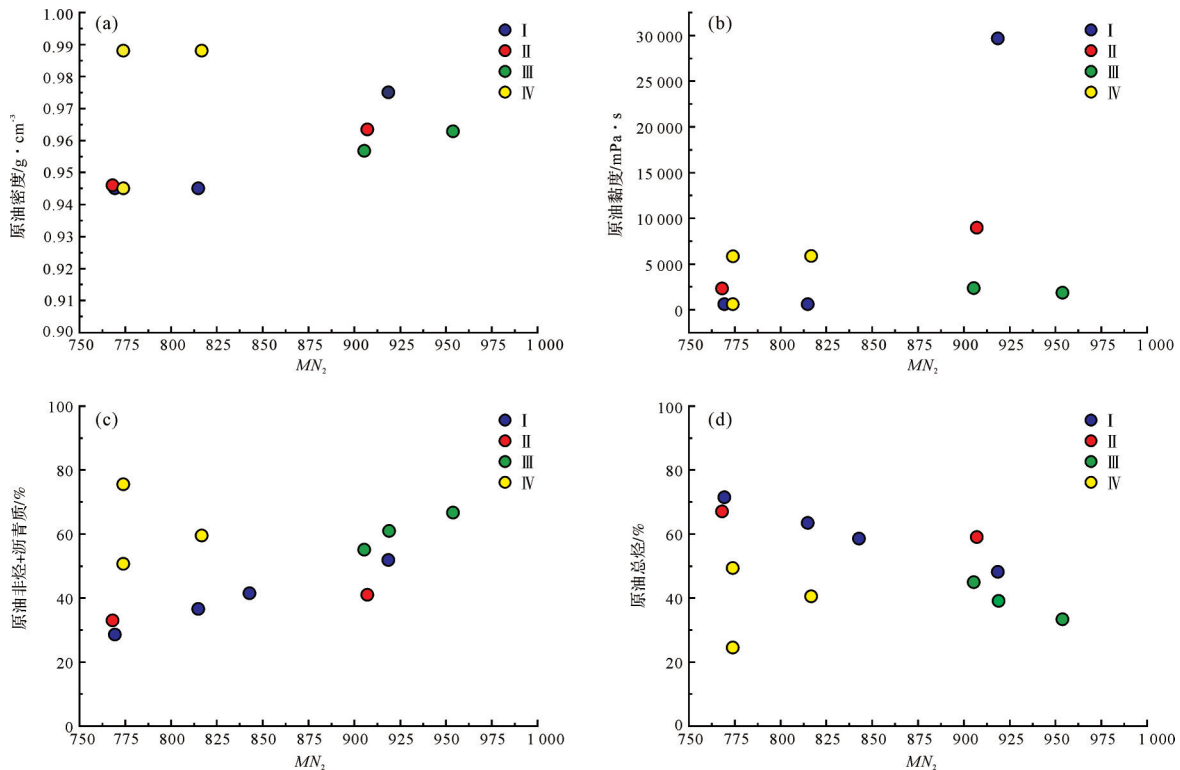


图5  $MN_2$ 值与密度(a)、黏度(b)、非烃和沥青质含量(c)、总烃(d)之间的相关关系  
Fig.5 Correlation of  $MN_2$  with (a) oil density; (b) oil viscosity; (c) non-hydrocarbon and asphaltene content; and (d) total hydrocarbon

事实上,原油黏度和Manco数之间并不是简单的线性关系<sup>[6]</sup>。生物降解以外的过程,即二次充注、水洗、混合多种成熟度充注以及重油中轻馏分的损失均可能导致油的黏度和API比重发生变化<sup>[23]</sup>。造成这种情况的原因可能是存在两期来源相同的石油充注,早期生物降解石油与后期石油混杂<sup>[9-10]</sup>。此外,埋藏

深度变化导致的保存条件差异通常也是影响生物降解的因素之一。

可见,PM法及优化的Manco法得出了较为一致的结论,成功厘定了生物降解程度在PM7-PM9+的样品: I<sub>1</sub>类、II<sub>1</sub>类、I<sub>2</sub>类、IV类、II<sub>2</sub>类、III<sub>1</sub>类、III<sub>2</sub>类原油的生物降解程度依次增强。



### 3.5 地球化学意义

PM法和优化Manco法具有一致性,但相比PM法,优化Manco法对原油生物降解的划分分辨率更高,可以区分PM等级相同但原油黏度不同的超稠油的生物降解程度,以了解相关样品之间生物降解过程程度的相对差异。与Larter *et al.*<sup>[6]</sup>创建的Manco等级(通常与PM等级4~8相关)相比,优化Manco法能够评价生物降解PM等级0~10的储层样品,是涵盖全区间的生物降解评价方法,适用于发生严重生物降解的原油生物降解程度评价。但本次优化的Manco法也存一些不足,如IV类原油中P1井(757 m)和P1井(761.6 m)的样品原油物性参数不同,但求得的 $MN_2$ 值相近,优化过程尚需进一步探索。

车排子凸起中生界稠油生物降解程度极高,稠油的黏度显示出数量级的变化,通过PM法定性评价和优化Manco法定量评价相结合,可以很好地揭示原油密度和黏度的变化,生物降解等级评价对深化油气藏的认识和勘探策略调整都有帮助。

## 4 结论

(1) 车排子凸起中生界侏罗系和白垩系原油均为重质稠油,非烃和沥青质含量较高。通过聚类分析,可以将车排子凸起东部的原油分为I、II、III、IV四类油族。按照原油降解程度的差异,不同原油族群还可以细分为不同组群。如I类原油可划分为 $I_1$ 类原油和 $I_2$ 类原油;II类原油可划分为 $II_1$ 类原油和 $II_2$ 类原油;III类原油可划分为 $III_1$ 类原油和 $III_2$ 类原油。

(2) PM法定性评价表明中生界原油降解程度可达PM7~PM9+。 $I_1$ 类原油生物降解程度为PM7, $I_2$ 类原油生物降解程度为PM8; $II_1$ 类原油生物降解程度为PM7, $II_2$ 类原油生物降解程度为PM9; $III_1$ 类原油生物降解程度为PM9, $III_2$ 类原油生物降解程度定PM9+;IV类原油生物降解程度为PM8。PM分析结果表明 $I_1$ 类、 $II_1$ 类、 $I_2$ 类、IV类、 $II_2$ 类、 $III_1$ 类、 $III_2$ 类原油的生物降解程度依次增强。

(3) 基于优化的Manco法求得的 $MN_1$ 值取值范围在19 693~215 623, $MN_2$ 值取值范围在768~954, $I_1$ 类原油的 $MN_2$ 值介于769~919, $II_1$ 类原油的 $MN_2$ 值介于768~907, $III_1$ 类原油的 $MN_2$ 值介于906~954,IV类原油的 $MN_2$ 值介于774~817。在同一原油族群内,Manco数与原油密度、黏度、非烃和沥青质含量均呈

现良好的正相关性。优化的Manco法成功厘定了生物降解程度在PM7~PM9+的储层样品,与PM等级评价具有一致性且有着更高的分辨率,它可以区分具有相同PM等级但原油黏度不同的样品,还可以进一步了解样品之间生物降解过程的相对差异。将PM法定性评价和优化Manco法定量评价相结合,可以很好地揭示原油物性的变化,对稠油区的油气勘探具有重要的指导作用。

致谢 感谢审稿专家和编辑老师对本文提出的修改意见。

### 参考文献(References)

- [1] Head I M, Jones D M, Larter S R. Biological activity in the deep subsurface and the origin of heavy oil[J]. *Nature*, 2003, 426 (6964): 344-352.
- [2] Meredith W, Kelland S J, Jones D M. Influence of biodegradation on crude oil acidity and carboxylic acid composition[J]. *Organic Geochemistry*, 2000, 31(11): 1059-1073.
- [3] Peters K E, Moldowan J M. The biomarker guide: Interpreting molecular fossils in petroleum and ancient sediments[M]. Englewood Cliffs, NJ: Prentice Hall, 1993: 363.
- [4] Volkman J K, Alexander R, Kagi R I, et al. Biodegradation of aromatic hydrocarbons in crude oils from the Barrow sub-basin of western Australia[J]. *Organic Geochemistry*, 1984, 6: 619-632.
- [5] Wenger L M, Isaksen G H. Control of hydrocarbon seepage intensity on level of biodegradation in sea bottom sediments[J]. *Organic Geochemistry*, 2002, 33(12): 1277-1292.
- [6] Larter S, Huang H P, Adams J, et al. A practical biodegradation scale for use in reservoir geochemical studies of biodegraded oils [J]. *Organic Geochemistry*, 2012, 45: 66-76.
- [7] Chang X C, Shi B B, Liu Z Q, et al. Investigation on the biodegradation levels of super heavy oils by parameter-stripping method and refined Manco scale: A case study from the Chepaizi uplift of Junggar Basin[J]. *Petroleum Science*, 2021, 18(2): 380-397.
- [8] 胡秋媛,董大伟,赵利,等. 准噶尔盆地车排子凸起构造演化特征及其成因[J]. *石油与天然气地质*, 2016, 37(4): 556-564. [Hu Qiuyuan, Dong Dawei, Zhao Li, et al. Tectonic evolutionary characteristics and their causes of Chepaizi uplift in Junggar Basin[J]. *Oil & Gas Geology*, 2016, 37(4): 556-564.]
- [9] Chang X C, Wang Y, Shi B B, et al. Charging of Carboniferous volcanic reservoirs in the eastern Chepaizi uplift, Junggar Basin (northwestern China) constrained by oil geochemistry and fluid inclusion[J]. *AAPG Bulletin*, 2019, 103(7): 1625-1652.
- [10] Shi B B, Chang X C, Xu Y D, et al. Charging history and fluid evolution for the Carboniferous volcanic reservoirs in the western Chepaizi uplift of Junggar Basin as determined by fluid inclusions and basin modelling[J]. *Geological Journal*, 2020, 55(4): 2591-2614.

- [11] Xu Y D, Chang X C, Shi B B, et al. Geochemistry of severely biodegraded oils in the Carboniferous volcanic reservoir of the Chepaizi uplift, Junggar Basin, NW China[J]. *Energy Exploration & Exploitation*, 2018, 36(6): 1461-1481.
- [12] 李阳. 准噶尔盆地车排子凸起东翼石炭系稠油地球化学与稠化机理研究[D]. 青岛: 山东科技大学, 2018. [Li Yang. Geochemistry and genetic mechanism of heavy oil in the eastern Chepaizi uplift, Junggar Basin[D]. Qingdao: Shandong University of Science and Technology, 2018. ]
- [13] 张枝焕, 向奎, 秦黎明, 等. 准噶尔盆地四棵树凹陷烃源岩地球化学特征及其对车排子凸起油气聚集的贡献[J]. *中国地质*, 2012, 39(2): 326-337. [Zhang Zhihuan, Xiang Kui, Qin Liming, et al. Geochemical characteristics of source rocks and their contribution to petroleum accumulation of Chepaizi area in Sikeshu Depression, Junggar Basin[J]. *Geology in China*, 2012, 39(2): 326-337. ]
- [14] Shi B B, Chang X C, Xu Y D, et al. Origin and migration pathway of biodegraded oils pooled in multiple-reservoirs of the Chepaizi uplift, Junggar Basin, NW China: Insights from geochemical characterization and chemometrics method[J]. *Marine and Petroleum Geology*, 2020, 122: 104655.
- [15] 沈扬, 贾东, 宋国奇, 等. 源外地区油气成藏特征、主控因素及地质评价: 以准噶尔盆地西缘车排子凸起春光油田为例[J]. *地质论评*, 2010, 56(1): 51-59. [Shen Yang, Jia Dong, Song Guoqi, et al. Reservoir-forming characters, key control factors and geological evaluation in the area outside oil source: Take the Chunguang oilfield in Chepaizi uplift in western Junggar Basin as an example[J]. *Geological Review*, 2010, 56(1): 51-59. ]
- [16] 牛靖靖. 准西车排子地区中生界油气成藏主控因素分析[D]. 青岛: 中国石油大学(华东), 2015. [Niu Jingjing. Analysis on main controlling factors of Mesozoic hydrocarbon accumulation in Chepaizi area of west Junggar Basin[D]. Qingdao: China University of Petroleum (East China), 2015. ]
- [17] Peters K E, Walters C C, Moldowan J M. *The biomarker guide: Biomarkers and isotopes in petroleum exploration and earth history*[M]. 2nd ed. New York: Cambridge University Press, 2005: 222-223.
- [18] Wang G L, Wang T G, Simoneit B R T, et al. Investigation of hydrocarbon biodegradation from a downhole profile in Bohai Bay Basin: Implications for the origin of 25-norhopanes[J]. *Organic Geochemistry*, 2013, 55: 72-84.
- [19] Chang X C, Wang G L, Guo H H, et al. A case study of crude oil alteration in a clastic reservoir by waterflooding[J]. *Journal of Petroleum Science and Engineering*, 2016, 146: 380-391.
- [20] Larter S, Wilhelms A, Head I, et al. The controls on the composition of biodegraded oils in the deep subsurface: Part 1: Biodegradation rates in petroleum reservoirs[J]. *Organic Geochemistry*, 2003, 34(4): 601-613.
- [21] López L, Mónaco S L, Volkman J K. Evidence for mixed and biodegraded crude oils in the Socororo field, eastern Venezuela Basin[J]. *Organic Geochemistry*, 2015, 82: 12-21.
- [22] 常象春, 孙婷婷, 王悦, 等. 水驱原油组分蚀变的地球化学响应及控制因素[J]. *地球科学与环境学报*, 2017, 39(6): 807-825. [Chang Xiangchun, Sun Tingting, Wang Yue, et al. Geochemical alteration of waterflooded oils and the controlling factors[J]. *Journal of Earth Sciences and Environment*, 2017, 39(6): 807-825. ]
- [23] López L. Study of the biodegradation levels of oils from the Orinoco Oil Belt (Junin area) using different biodegradation scales [J]. *Organic Geochemistry*, 2014, 66: 60-69.

## Evaluation of the Biodegradation of Mesozoic Crude Oils in the Eastern Chepaizi Uplift

SU Lei<sup>1</sup>, CHANG XiangChun<sup>1</sup>, XU YouDe<sup>2</sup>, LIU ZhongQuan<sup>2</sup>, SHI BingBing<sup>1</sup>

1. College of Earth Science and Engineering, Shandong University of Science and Technology, Qingdao, Shandong 266590, China

2. Institute of Petroleum Exploration and Development, Shengli Oilfield Company, SINOPEC, Dongying, Shandong 257015, China

**Abstract:** [Objective] Biodegraded crude oil is commonly found in poriferous basins globally. Biodegradation will have a profound impact on the physical properties and group components of crude oil, resulting in an increase in the oil density and viscosity, an enrichment in the non-hydrocarbon, asphaltene, sulfur metallic ion content and acid value. In recent years, the Mesozoic (Jurassic and Cretaceous) oil-bearing sandstone reservoirs in the east margin of the Chepaizi uplift have attracted much more attention due to the discovery of large quantities of crude oil, but their severe biodegradation restricts the exploration process. In order to clarify the biodegradation level of Mesozoic crude oil in the east margin of the Chepaizi uplift, the saturated hydrocarbon and the aromatic hydrocarbon fractions extracted from the reservoir samples from 10 wells in the Mesozoic east margin of Chepaizi uplift were analyzed by gas chromatography-mass spectrometry (GC-MS), and molecular biomarkers strongly resistant to biodegradation were investigated. [Methods] Cluster analysis, a statistical method, is an effective tool to classify studied samples into different groups by their similarity distances which were calculated from the different variables investigated. Allowing for the severe oil alteration, the following nine biomarker parameters related to tricyclic terpenes (TT), tetracyclic terpenes (Tet) and triaromatic steranes (TAS) with strong biodegradation resistance were selected:  $(C_{19}TT + C_{20}TT) / (C_{23}TT + C_{24}TT)$ ,  $C_{19}TT/C_{23}TT$ ,  $C_{23}TT/C_{21}TT$ ,  $C_{22}TT/C_{21}TT$ ,  $C_{24}TT/C_{23}TT$ , ETR,  $C_{24}Tet/C_{26}TT$ ,  $C_{27}TAS/C_{28}TAS$  (20R),  $C_{26}TAS/C_{28}TAS$  (20S). Cluster analysis (HCA) was performed to classify the Mesozoic crude oil populations. On this basis, the biodegradation level of Mesozoic crude oil was qualitatively evaluated according to the PM (Peters and Moldowan) method and descriptive terms. Then, following the academic theory of Manco scale, eight compounds with different sensitivities to microbial degradation, which characterize progressive bioresistance, were selected. Variables were assigned for them to optimize the quantitative evaluation scale of Manco method. The parametric vectors of the eight compounds generally covered the whole degradation level (PM0 ~ PM10), including (1) n-alkanes ( $m/z$  85); (2) naphthalene and alkyl naphthalene ( $m/z$  128, 142, 156, 170, 184, 198); (3) alkyl dibenzothiophene ( $m/z$  198, 212, 226); (4)  $C_{0-3}$  phenanthrene ( $m/z$  178, 192, 206, 220); (5) pentacyclic triterpenes ( $m/z$  191, 177, 205); (6) sterane ( $m/z$  217, 218, 259); (7) tricyclic terpenoids ( $m/z$  191, 177); and (8) triaromatic steroids ( $m/z$  231, 245).  $MN_1$  (Manco Number 1) and  $MN_2$  (Manco Number 2) were calculated by the formulas, and the correlation between them and crude oil properties was analyzed. [Results and Discussions] The result shows that the Mesozoic crude oil is a typical heavy oil with high density and high viscosity, especially the viscosity of crude oil shows an order of magnitude change, which essentially reflects the alteration effect of microbial degradation. The oil density showed roughly positive correlation with the viscosity and the NSO (resin + asphaltene) fraction content, and negative correlation with the burial depth. Progressive biodegradation of crude oils may be responsible. The results of cluster analysis shows that the Mesozoic crude oil in the eastern Chepaizi uplift can be divided into four oil populations, i.e., I, II, III and IV. According to the difference of crude oil degradation level, different crude oil groups can be subdivided into different families. For example, group I crude oil is subdivided into family I<sub>1</sub> crude oil (well P1, 781.5 m and 721.5 m) with a biodegradation level of PM7 (heavy) and family I<sub>2</sub> crude oil (wells P607 and P624) with a biodegradation level of PM8 (very heavy). Group II is subdivided into family II<sub>1</sub> crude oil (well P1, 748.5 m

and 751.2 m) with a biodegradation level of PM7 (heavy) and family II<sub>2</sub> crude oil (wells P60 and P604) with a biodegradation level of PM9 (very heavy). Group III is subdivided into family III<sub>1</sub> crude oil (wells P629, P68, and P606) with a biodegradation level of PM9 (very heavy) and family III<sub>2</sub> crude oil (well P646) with a biodegradation level of PM9+ (severe). Group IV includes well P1 (756.8 m, 757 m, 761.6 m, and 766.5 m) and well P609, and the biodegradation level of group IV is PM8 (very heavy). Qualitative evaluation result by the PM method shows that the degradation level of Mesozoic crude oil can reach PM7-PM9+. The  $MN_1$  value obtained by the optimized Manco method ranges from 19 693 to 215 623; the  $MN_2$  value obtained by the optimized Manco method ranges from 768 to 954. For a single oil population, the values of  $MN_1$  and  $MN_2$  increased with the biodegradation level. In addition, the Manco number shows a good positive correlation with oil density, viscosity, non-hydrocarbon and asphaltene content, and a good negative correlation with total hydrocarbon content. The exception is the oil from well P646, which has a higher level of biodegradation than well P606 but shows a lower viscosity. Factually, there is not a simple relationship between the oil viscosity and the Manco number. Processes other than biodegradation, i.e., secondary oil charge, water washing, mixing of multiple maturity oil charges, and loss of light ends from heavy oils could produce variations in oil viscosity and density. The two episodes of oil charging, early biodegraded oils mixed with the later re-migration of preexisting oils due to the structural adjustment, yet the same oil origin in the Chepaizi uplift maybe responsible for this case. In addition, differences in preservation conditions due to changes in burial depth can be one of the factors affecting biodegradation. [Conclusions] The optimized Manco method successfully distinguishes the oil-bearing reservoir samples with biodegradation level in PM7-PM9+, which is consistent with the PM result, that is, the biodegradation level of family I<sub>1</sub>, family II<sub>1</sub>, family I<sub>2</sub>, group IV, family II<sub>2</sub>, family III<sub>1</sub>, family III<sub>2</sub> successively increases. In addition, the optimized Manco method provides a more detailed classification than the PM method, because it can clearly distinguish crude oil with the same PM level but different crude oil physical properties. This way, the differences in the biodegradation of oil-bearing reservoir samples can be clearly shown. The combination of qualitative evaluation by the PM method and quantitative evaluation by the optimized Manco method can reveal the difference in crude oil physical properties, which plays a guiding role for oil and gas exploration in this area.

**Key words:** biodegradation; PM method; optimized Manco method; Mesozoic; Chepaizi uplift